

# Corrections to $R_D$ and $R_{D^*}$ in the BLMSSM<sup>\*</sup>

Zhong-Jun Yang(杨忠军)<sup>1)</sup> Shu-Min Zhao(赵树民)<sup>2)</sup> Xing-Xing Dong(董幸幸)<sup>3)</sup>

Xi-Jie Zhan(展希杰) Hai-Bin Zhang(张海斌) Tai-Fu Feng(冯太傅)

National-Local Joint Engineering Laboratory of New Energy Photoelectric Devices, Department of Physics, Hebei University, Baoding 071002, China

**Abstract:** The deviation of the measurement of  $R_D$  ( $R_{D^*}$ ) from the Standard Model (SM) expectation is  $2.3\sigma$  ( $3.1\sigma$ ).  $R_D$  ( $R_{D^*}$ ) is the ratio of the branching fraction of  $\overline{B} \rightarrow D\tau\overline{\nu}_\tau$  ( $\overline{B} \rightarrow D^*\tau\overline{\nu}_\tau$ ) to that of  $\overline{B} \rightarrow D l\overline{\nu}_l$  ( $\overline{B} \rightarrow D^* l\overline{\nu}_l$ ), where  $l=e$  or  $\mu$ . This anomaly may imply the existence of new physics (NP). In this paper, we restudy this problem in the supersymmetric extension of the Standard Model with local gauged baryon and lepton numbers (BLMSSM), and give one-loop corrections to  $R_D$  ( $R_{D^*}$ ).

**Keywords:** supersymmetry, BLMSSM, semileptonic decay

**PACS:** 12.60.Jv, 13.30.Ce **DOI:** 10.1088/1674-1137/42/11/113104

## 1 Introduction

The Standard Model (SM) is the most successful particle physics model to date. It gives accurate predictions for a significant number of experiments. However, for some experiments, it cannot give a good explanation. In the last few years, the experimental measurements of  $R_{D^{(*)}}$  (the ratio of the branching fraction of  $\overline{B} \rightarrow D\tau\overline{\nu}_\tau$  ( $\overline{B} \rightarrow D^*\tau\overline{\nu}_\tau$ ) to that of  $\overline{B} \rightarrow D l\overline{\nu}_l$  ( $\overline{B} \rightarrow D^* l\overline{\nu}_l$ ), where  $l=e$  or  $\mu$ ) show deviations from the SM theoretical predictions – these measurements are larger than SM expectations. Therefore, in order to explain these anomalies, it is necessary for us to try some new physics (NP) models.

The SM expectations for  $R_{D^{(*)}}$  are:  $R_{D_{SM}} = 0.299 \pm 0.011$  in Ref. [1],  $R_{D_{SM}} = 0.299 \pm 0.003$  in Ref. [2],  $R_{D_{SM}} = 0.300 \pm 0.008$  in Ref. [3],  $R_{D_{SM}} = 0.300 \pm 0.011$  in Ref. [4],  $R_{D_{SM}} = 0.299 \pm 0.003$  in Ref. [5],  $R_{D^*_{SM}} = 0.254 \pm 0.004$  in Ref. [4],  $R_{D^*_{SM}} = 0.257 \pm 0.003$  in Ref. [5] and  $R_{D^*_{SM}} = 0.252 \pm 0.003$  in Ref. [6]. The relevant experimental results for  $R_{D^{(*)}}$  are listed in Table 1.

$R_D = 0.407 \pm 0.039 \pm 0.024$  and  $R_{D^*} = 0.304 \pm 0.013 \pm 0.007$  exceed the SM predictions by  $2.3\sigma$  and  $3.1\sigma$  respectively. These anomalies have caused physicists to seek a variety of ways to explain the experimental data [15–35]. Most physicists tend to seek the solutions in NP models. So, various NP models have been used, such as charged Higgs

[30–32] and lepton flavor violation [33–35]. The supersymmetric extension of the SM is a popular choice in various NP models. In fact, theorists have been fond of the minimal supersymmetric model (MSSM) for a long time. However, baryon number (B) should be broken because of the matter-antimatter asymmetry in the Universe. The neutrino oscillation experiments imply that neutrinos have tiny masses, therefore lepton number (L) also needs to be broken. A minimal supersymmetric extension of the SM with local gauged B and L (BLMSSM) [36, 37] is more promising. Thus, we try to deal with the anomalies of  $R_{D^{(*)}}$  in the BLMSSM.

In our work, we use effective field theory to do the theoretical calculation. The effective Lagrangian is described by the four fermion operators and the corresponding Wilson coefficients (WCs). NP contributions with non-zero WCs are possible solutions to the  $R_{D^{(*)}}$  anomalies [38]. After considering all the 10 independent 6-dimensional operators and calculating the values of the corresponding WCs at one-loop level, we obtain the theoretical values of  $R_{D^{(*)}}$  in the BLMSSM.

This paper is organised as follows. In Section 2, we introduce some content of the BLMSSM. In Section 3, we give the mass matrices of the BLMSSM particles that we use. In Section 4, we write down the needed couplings. In Section 5, we provide the relevant formulae, including

Received 19 June 2018, Revised 19 August 2018, Published online 13 October 2018

\* Supported by the NNSFC (11535002, 11605037, 11705045), the Natural Science Foundation of Hebei Province (A2016201010, A2016201069), the Natural Science Fund of Hebei University (2011JQ05, 2012-242), and Hebei Key Lab of Opto-Electronic Information and Materials, the Midwest Universities Comprehensive Strength Promotion Project

1) E-mail: zj\_yang1993@163.com

2) E-mail: zhaosm@hbu.edu.cn

3) E-mail: dxx\_0304@163.com



Content from this work may be used under the terms of the Creative Commons Attribution 3.0 licence. Any further distribution of this work must maintain attribution to the author(s) and the title of the work, journal citation and DOI. Article funded by SCOAP<sup>3</sup> and published under licence by Chinese Physical Society and the Institute of High Energy Physics of the Chinese Academy of Sciences and the Institute of Modern Physics of the Chinese Academy of Sciences and IOP Publishing Ltd

observables  $R_{D^{(*)}}$  and the effective Lagrangian with all the four fermion operators. In Section 6, we show the one-loop Feynman diagrams that can correct  $R_{D^{(*)}}$ . At the same time, NP contributions of some diagrams are given by WCs. In Section 7, we present our numerical results. Finally, we summarise our findings in Section 8. Some integral formulae are shown in the Appendix.

 Table 1. The measurements of  $R_{D^{(*)}}$ .

observable	experiment	measured value
$R_D$	2012 BaBar	$0.440 \pm 0.058 \pm 0.042$ [7, 8]
	2015 Belle	$0.375 \pm 0.064 \pm 0.026$ [9]
	2017 HFAG average	$0.407 \pm 0.039 \pm 0.024$ [10]
$R_{D^*}$	2012 BaBar	$0.332 \pm 0.024 \pm 0.018$ [7, 8]
	2015 Belle	$0.293 \pm 0.038 \pm 0.015$ [9]
	2015 LHCb	$0.336 \pm 0.027 \pm 0.030$ [11]
	2016 Belle	$0.302 \pm 0.030 \pm 0.011$ [12]
	2017 Belle	$0.270 \pm 0.035^{+0.028}_{-0.025}$ [13]
	2017 LHCb	$0.291 \pm 0.019 \pm 0.026 \pm 0.013$ [14]
	2017 HFAG average	$0.304 \pm 0.013 \pm 0.007$ [10]

## 2 Some content of the BLMSSM

As an extension of the MSSM, the BLMSSM includes many new fields [39, 40]. The exotic quarks ( $\hat{Q}_4, \hat{U}_4^c, \hat{D}_4^c, \hat{Q}_5^c, \hat{U}_5^c, \hat{D}_5^c$ ) are used to deal with the B

anomaly. The exotic leptons ( $\hat{L}_4, \hat{E}_4^c, \hat{N}_4^c, \hat{L}_5^c, \hat{E}_5^c, \hat{N}_5^c$ ) are used to cancel the L anomaly. The exotic Higgs superfields  $\hat{\Phi}_B, \hat{\varphi}_B$  are introduced to break baryon number spontaneously with non-zero vacuum expectation values (VEVs). The exotic Higgs superfields  $\hat{\Phi}_L, \hat{\varphi}_L$  are introduced to break lepton number spontaneously with non-zero VEVs. The model introduces the right-handed neutrinos  $N_R^c$ , so we can obtain tiny masses of neutrinos through the see-saw mechanism. The model also includes the superfields  $\hat{X}$  to make the exotic quarks unstable.

The superpotential of the BLMSSM is [41]:

$$\begin{aligned}
 \mathcal{W}_{\text{BLMSSM}} &= \mathcal{W}_{\text{MSSM}} + \mathcal{W}_B + \mathcal{W}_L + \mathcal{W}_X, \\
 \mathcal{W}_B &= \lambda_Q \hat{Q}_4 \hat{Q}_5^c \hat{\Phi}_B + \lambda_U \hat{U}_4^c \hat{U}_5^c \hat{\varphi}_B + \lambda_D \hat{D}_4^c \hat{D}_5^c \hat{\varphi}_B \\
 &\quad + \mu_B \hat{\Phi}_B \hat{\varphi}_B + Y_{u_4} \hat{Q}_4 \hat{H}_u \hat{U}_4^c + Y_{d_4} \hat{Q}_4 \hat{H}_d \hat{D}_4^c \\
 &\quad + Y_{u_5} \hat{Q}_5^c \hat{H}_d \hat{U}_5^c + Y_{d_5} \hat{Q}_5^c \hat{H}_u \hat{D}_5^c, \\
 \mathcal{W}_L &= Y_{e_4} \hat{L}_4 \hat{H}_d \hat{E}_4^c + Y_{\nu_4} \hat{L}_4 \hat{H}_u \hat{N}_4^c + Y_{e_5} \hat{L}_5^c \hat{H}_u \hat{E}_5^c \\
 &\quad + Y_{\nu_5} \hat{L}_5^c \hat{H}_d \hat{N}_5^c + Y_\nu \hat{L} \hat{H}_u \hat{N}^c + \lambda_{N^c} \hat{N}^c \hat{N}^c \hat{\varphi}_L \\
 &\quad + \mu_L \hat{\Phi}_L \hat{\varphi}_L, \\
 \mathcal{W}_X &= \lambda_1 \hat{Q} \hat{Q}_5^c \hat{X} + \lambda_2 \hat{U}^c \hat{U}_5^c \hat{X}' + \lambda_3 \hat{D}^c \hat{D}_5^c \hat{X}' + \mu_X \hat{X} \hat{X}', \tag{1}
 \end{aligned}$$

where  $\mathcal{W}_{\text{MSSM}}$  is the superpotential of the MSSM.

The soft breaking terms  $\mathcal{L}_{\text{soft}}$  of the BLMSSM can be written in the following form [36, 37, 41]:

$$\begin{aligned}
 \mathcal{L}_{\text{soft}} &= \mathcal{L}_{\text{soft}}^{\text{MSSM}} - (m_{\nu^c}^2)_{IJ} \tilde{N}_I^{c*} \tilde{N}_J^c - m_{\tilde{Q}_4}^2 \tilde{Q}_4^\dagger \tilde{Q}_4 - m_{\tilde{U}_4}^2 \tilde{U}_4^* \tilde{U}_4^c - m_{\tilde{D}_4}^2 \tilde{D}_4^{c*} \tilde{D}_4^c \\
 &\quad - m_{\tilde{Q}_5}^2 \tilde{Q}_5^{c\dagger} \tilde{Q}_5^c - m_{\tilde{U}_5}^2 \tilde{U}_5^* \tilde{U}_5^c - m_{\tilde{D}_5}^2 \tilde{D}_5^* \tilde{D}_5^c - m_{\tilde{L}_4}^2 \tilde{L}_4^\dagger \tilde{L}_4 - m_{\tilde{\nu}_4}^2 \tilde{N}_4^{c*} \tilde{N}_4^c \\
 &\quad - m_{\tilde{e}_4}^2 \tilde{E}_4^{c*} \tilde{E}_4^c - m_{\tilde{L}_5}^2 \tilde{L}_5^{c\dagger} \tilde{L}_5^c - m_{\tilde{\nu}_5}^2 \tilde{N}_5^* \tilde{N}_5^c - m_{\tilde{e}_5}^2 \tilde{E}_5^* \tilde{E}_5^c - m_{\Phi_B}^2 \Phi_B^* \Phi_B \\
 &\quad - m_{\varphi_B}^2 \varphi_B^* \varphi_B - m_{\Phi_L}^2 \Phi_L^* \Phi_L - m_{\varphi_L}^2 \varphi_L^* \varphi_L - (M_B \lambda_B \lambda_B + M_L \lambda_L \lambda_L + h.c.) \\
 &\quad + \left\{ A_{u_4} Y_{u_4} \tilde{Q}_4 H_u \tilde{U}_4^c + A_{d_4} Y_{d_4} \tilde{Q}_4 H_d \tilde{D}_4^c + A_{u_5} Y_{u_5} \tilde{Q}_5^c H_d \tilde{U}_5^c + A_{d_5} Y_{d_5} \tilde{Q}_5^c H_u \tilde{D}_5^c \right. \\
 &\quad + A_{BQ} \lambda_Q \tilde{Q}_4 \tilde{Q}_5^c \Phi_B + A_{BU} \lambda_U \tilde{U}_4^c \tilde{U}_5^c \varphi_B + A_{BD} \lambda_D \tilde{D}_4^c \tilde{D}_5^c \varphi_B + B_B \mu_B \Phi_B \varphi_B + h.c. \left. \right\} \\
 &\quad + \left\{ A_{e_4} Y_{e_4} \tilde{L}_4 H_d \tilde{E}_4^c + A_{\nu_4} Y_{\nu_4} \tilde{L}_4 H_u \tilde{N}_4^c + A_{e_5} Y_{e_5} \tilde{L}_5^c H_u \tilde{E}_5^c + A_{\nu_5} Y_{\nu_5} \tilde{L}_5^c H_d \tilde{N}_5^c \right. \\
 &\quad + A_{\nu} Y_{\nu} \tilde{L} H_u \tilde{N}^c + A_{\nu^c} \lambda_{\nu^c} \tilde{N}^c \tilde{N}^c \varphi_L + B_L \mu_L \Phi_L \varphi_L + h.c. \left. \right\} \\
 &\quad + \left\{ A_1 \lambda_1 \tilde{Q} \tilde{Q}_5^c X + A_2 \lambda_2 \tilde{U}^c \tilde{U}_5^c X' + A_3 \lambda_3 \tilde{D}^c \tilde{D}_5^c X' + B_X \mu_X X X' + h.c. \right\}. \tag{2}
 \end{aligned}$$

The  $SU(2)_L$  singlets  $\Phi_L, \varphi_L, \Phi_B, \varphi_B$  and the  $SU(2)_L$  doublets  $H_u, H_d$  are:

$$\begin{aligned}
 \Phi_L &= \frac{1}{\sqrt{2}} \begin{pmatrix} v_L + \Phi_L^0 + iP_L^0 \\ \Phi_L^- \end{pmatrix}, & \varphi_L &= \frac{1}{\sqrt{2}} \begin{pmatrix} \bar{v}_L + \varphi_L^0 + i\bar{P}_L^0 \\ \varphi_L^- \end{pmatrix}, \\
 \Phi_B &= \frac{1}{\sqrt{2}} \begin{pmatrix} v_B + \Phi_B^0 + iP_B^0 \\ \Phi_B^- \end{pmatrix}, & \varphi_B &= \frac{1}{\sqrt{2}} \begin{pmatrix} \bar{v}_B + \varphi_B^0 + i\bar{P}_B^0 \\ \varphi_B^- \end{pmatrix}, \\
 H_u &= \begin{pmatrix} H_u^+ \\ \frac{1}{\sqrt{2}} (v_u + H_u^0 + iP_u^0) \end{pmatrix}, \\
 H_d &= \begin{pmatrix} \frac{1}{\sqrt{2}} (v_d + H_d^0 + iP_d^0) \\ H_d^- \end{pmatrix}. \tag{3}
 \end{aligned}$$

The  $SU(2)_L$  singlets  $\Phi_L, \varphi_L, \Phi_B, \varphi_B$  and the  $SU(2)_L$  doublets  $H_u, H_d$  should obtain non-zero VEVs  $v_L, \bar{v}_L, v_B, \bar{v}_B$  and  $v_u, v_d$  respectively. Therefore, the local gauge symmetry  $SU(2)_L \otimes U(1)_Y \otimes U(1)_B \otimes U(1)_L$  breaks down to the electromagnetic symmetry  $U(1)_e$ .

## 3 Mass matrices for some BLMSSM particles

Lepneutralinos are made up of  $\lambda_L$  (the superpartner of the new lepton boson), and  $\psi_{\Phi_L}$  and  $\psi_{\varphi_L}$  (the superpartners of the  $SU(2)_L$  singlets  $\Phi_L$  and  $\varphi_L$ ). The mass

mixing matrix of leptonneutralinos  $M_{LN}$  is shown in the basis  $(i\lambda_L, \psi_{\Phi_L}, \psi_{\varphi_L})$  [42–45].  $\chi_{L_i}^0$  ( $i = 1, 2, 3$ ) are mass eigenstates of leptonneutralinos. The masses of the three leptonneutralinos are obtained from diagonalizing  $M_{LN}$  by  $Z_{NL}$ :

$$M_{LN} = \begin{pmatrix} 2M_L & 2v_L g_L & -2\bar{v}_L g_L \\ 2v_L g_L & 0 & -\mu_L \\ -2\bar{v}_L g_L & -\mu_L & 0 \end{pmatrix},$$

$$i\lambda_L = Z_{NL}^{1i} k_{L_i}^0, \quad \psi_{\Phi_L} = Z_{NL}^{2i} k_{L_i}^0,$$

$$\psi_{\varphi_L} = Z_{NL}^{3i} k_{L_i}^0, \quad \chi_{L_i}^0 = \begin{pmatrix} k_{L_i}^0 \\ \bar{k}_{L_i}^0 \end{pmatrix}. \quad (4)$$

The slepton mass squared matrix becomes

$$\begin{pmatrix} (\mathcal{M}_{\tilde{L}}^2)_{LL} & (\mathcal{M}_{\tilde{L}}^2)_{LR} \\ (\mathcal{M}_{\tilde{L}}^2)_{LR}^\dagger & (\mathcal{M}_{\tilde{L}}^2)_{RR} \end{pmatrix}, \quad (5)$$

which is diagonalized by the matrix  $Z_{\tilde{L}}$ .  $(\mathcal{M}_{\tilde{L}}^2)_{LL}$ ,  $(\mathcal{M}_{\tilde{L}}^2)_{LR}$  and  $(\mathcal{M}_{\tilde{L}}^2)_{RR}$  are:

$$(\mathcal{M}_{\tilde{L}}^2)_{LL} = \frac{(g_1^2 - g_2^2)(v_d^2 - v_u^2)}{8} \delta_{IJ} + g_L^2 (\bar{v}_L^2 - v_L^2) \delta_{IJ} + m_{\tilde{L}_I}^2 \delta_{IJ} + (m_{\tilde{L}}^2)_{IJ},$$

$$(\mathcal{M}_{\tilde{L}}^2)_{LR} = \frac{\mu^* v_u}{\sqrt{2}} (Y_I)_{IJ} - \frac{v_u}{\sqrt{2}} (A'_I)_{IJ} + \frac{v_d}{\sqrt{2}} (A_I)_{IJ},$$

$$(\mathcal{M}_{\tilde{L}}^2)_{RR} = \frac{g_1^2 (v_u^2 - v_d^2)}{4} \delta_{IJ} - g_L^2 (\bar{v}_L^2 - v_L^2) \delta_{IJ} + m_{\tilde{L}_I}^2 \delta_{IJ} + (m_{\tilde{R}}^2)_{IJ}. \quad (6)$$

The mass squared matrix of sneutrino  $\mathcal{M}_{\tilde{n}}$  with  $\tilde{n}^T = (\tilde{\nu}, \tilde{N}^c)$  reads [46]

$$\begin{pmatrix} \mathcal{M}_{\tilde{n}}^2(\tilde{\nu}_I^* \tilde{\nu}_J) & \mathcal{M}_{\tilde{n}}^2(\tilde{\nu}_I \tilde{N}_J^c) \\ (\mathcal{M}_{\tilde{n}}^2(\tilde{\nu}_I \tilde{N}_J^c))^\dagger & \mathcal{M}_{\tilde{n}}^2(\tilde{N}_I^{c*} \tilde{N}_J^c) \end{pmatrix}. \quad (7)$$

$\mathcal{M}_{\tilde{n}}^2(\tilde{\nu}_I^* \tilde{\nu}_J)$ ,  $\mathcal{M}_{\tilde{n}}^2(\tilde{\nu}_I \tilde{N}_J^c)$  and  $\mathcal{M}_{\tilde{n}}^2(\tilde{N}_I^{c*} \tilde{N}_J^c)$  are:

$$\mathcal{M}_{\tilde{n}}^2(\tilde{\nu}_I^* \tilde{\nu}_J) = \frac{g_1^2 + g_2^2}{8} (v_d^2 - v_u^2) \delta_{IJ} + g_L^2 (\bar{v}_L^2 - v_L^2) \delta_{IJ} + \frac{v_u^2}{2} (Y_\nu^\dagger Y_\nu)_{IJ} + (m_{\tilde{L}}^2)_{IJ},$$

$$\mathcal{M}_{\tilde{n}}^2(\tilde{\nu}_I \tilde{N}_J^c) = \mu^* \frac{v_d}{\sqrt{2}} (Y_\nu)_{IJ} - v_u \bar{v}_L (Y_\nu^\dagger \lambda_{N^c})_{IJ} + \frac{v_u}{\sqrt{2}} (A_N)_{IJ} (Y_\nu)_{IJ},$$

$$\mathcal{M}_{\tilde{n}}^2(\tilde{N}_I^{c*} \tilde{N}_J^c) = -g_L^2 (\bar{v}_L^2 - v_L^2) \delta_{IJ} + \frac{v_u^2}{2} (Y_\nu^\dagger Y_\nu)_{IJ} + 2\bar{v}_L^2 (\lambda_{N^c}^\dagger \lambda_{N^c})_{IJ} + (m_{\tilde{N}^c}^2)_{IJ} + \mu_L \frac{v_L}{\sqrt{2}} (\lambda_{N^c})_{IJ} - \frac{\bar{v}_L}{\sqrt{2}} (A_{N^c})_{IJ} (\lambda_{N^c})_{IJ}. \quad (8)$$

Then the masses of the sneutrinos are obtained by using the formula  $Z_{\tilde{\nu}}^\dagger \mathcal{M}_{\tilde{n}}^2 Z_{\tilde{\nu}} = \text{diag}(m_{\tilde{\nu}_1}^2, m_{\tilde{\nu}_2}^2, m_{\tilde{\nu}_3}^2, m_{\tilde{\nu}_4}^2, m_{\tilde{\nu}_5}^2, m_{\tilde{\nu}_6}^2)$ .

The up scalar quark mass squared matrix in the BLMSSM is given by

$$\begin{pmatrix} (\mathcal{M}_{\tilde{U}}^2)_{LL} & (\mathcal{M}_{\tilde{U}}^2)_{LR} \\ (\mathcal{M}_{\tilde{U}}^2)_{LR}^\dagger & (\mathcal{M}_{\tilde{U}}^2)_{RR} \end{pmatrix}, \quad (9)$$

which is diagonalized by the matrix  $Z_{\tilde{U}}$ .  $(\mathcal{M}_{\tilde{U}}^2)_{LL}$ ,  $(\mathcal{M}_{\tilde{U}}^2)_{LR}$  and  $(\mathcal{M}_{\tilde{U}}^2)_{RR}$  are:

$$(\mathcal{M}_{\tilde{U}}^2)_{LL} = -\frac{e^2(v_d^2 - v_u^2)(1 - 4c_W^2)}{24s_W^2 c_W^2} + \frac{v_u^2 Y_u^2}{2} + (K m_Q^2 K^\dagger)^T + \frac{g_B^2}{6} (v_B^2 - \bar{v}_B^2),$$

$$(\mathcal{M}_{\tilde{U}}^2)_{RR} = \frac{e^2(v_d^2 - v_u^2)}{6c_W^2} + \frac{v_u^2 Y_u^2}{2} + m_{\tilde{U}}^2 - \frac{g_B^2}{6} (v_B^2 - \bar{v}_B^2),$$

$$(\mathcal{M}_{\tilde{U}}^2)_{LR} = -\frac{1}{\sqrt{2}} (v_d(A'_u + Y_u \mu^*) + v_u A_u). \quad (10)$$

The down scalar quark mass squared matrix in the BLMSSM is given by

$$\begin{pmatrix} (\mathcal{M}_{\tilde{D}}^2)_{LL} & (\mathcal{M}_{\tilde{D}}^2)_{LR} \\ (\mathcal{M}_{\tilde{D}}^2)_{LR}^\dagger & (\mathcal{M}_{\tilde{D}}^2)_{RR} \end{pmatrix}, \quad (11)$$

which is diagonalized by the matrix  $Z_{\tilde{D}}$ .  $(\mathcal{M}_{\tilde{D}}^2)_{LL}$ ,  $(\mathcal{M}_{\tilde{D}}^2)_{LR}$  and  $(\mathcal{M}_{\tilde{D}}^2)_{RR}$  are:

$$(\mathcal{M}_{\tilde{D}}^2)_{LL} = -\frac{e^2(v_d^2 - v_u^2)(1 + 2c_W^2)}{24s_W^2 c_W^2} + \frac{v_d^2 Y_d^2}{2} + (m_Q^2)^T + \frac{g_B^2}{6} (v_B^2 - \bar{v}_B^2),$$

$$(\mathcal{M}_{\tilde{D}}^2)_{RR} = -\frac{e^2(v_d^2 - v_u^2)}{12c_W^2} + \frac{v_d^2 Y_d^2}{2} + m_{\tilde{D}}^2 - \frac{g_B^2}{6} (v_B^2 - \bar{v}_B^2),$$

$$(\mathcal{M}_{\tilde{D}}^2)_{LR} = \frac{1}{\sqrt{2}} (v_u(-A'_d + Y_d \mu^*) + v_d A_d). \quad (12)$$

In the basis  $(\psi_{\nu_L^I}, \psi_{N_R^{cI}})$ , the neutrino mass mixing matrix is diagonalized by  $Z_\nu$  [46]:

$$Z_\nu^T \begin{pmatrix} 0 & \frac{v_u}{\sqrt{2}} (Y_\nu)_{IJ} \\ \frac{v_u}{\sqrt{2}} (Y_\nu^T)_{IJ} & \frac{\bar{v}_L}{\sqrt{2}} (\lambda_{N^c})_{IJ} \end{pmatrix} Z_\nu = \text{diag}(m_{\nu^\alpha}), \quad \alpha = 1 \dots 6.$$

$$\psi_{\nu_L^I} = Z_\nu^{I\alpha} k_{N\alpha}^0, \quad \psi_{N_R^{cI}} = Z_\nu^{(I+3)\alpha} k_{N\alpha}^0,$$

$$\nu^\alpha = \begin{pmatrix} k_{N\alpha}^0 \\ \bar{k}_{N\alpha}^0 \end{pmatrix}. \quad (13)$$

$\nu^\alpha$  denotes the mass eigenstates of the neutrino fields mixed by the left-handed and right-handed neutrinos. In this paper, we deal with the neutrinos by an approximation,  $Z_\nu \approx 1$ , so the theoretical values at tree level are consistent with those in the SM.

## 4 Necessary couplings

In the BL MSSM, due to the superfields  $\tilde{N}^c$ , we deduce the corrections to the couplings in the MSSM. The couplings for  $W$ - $l$ - $\nu$  and  $W$ - $\tilde{L}$ - $\tilde{\nu}$  read

$$\mathcal{L}_{Wl\nu} = -\frac{e}{\sqrt{2}s_W} W_\mu^+ \sum_{I=1}^3 \sum_{\alpha=1}^6 Z_\nu^{I\alpha*} \bar{\nu}^\alpha \gamma^\mu P_L l^I, \quad (14)$$

$$\mathcal{L}_{W\tilde{L}\tilde{\nu}} = -\frac{i\tilde{e}}{\sqrt{2}s_W} W_\mu^- \sum_{I=1}^3 \sum_{i,\alpha=1}^6 (Z_{\tilde{L}}^{Ii} Z_{\tilde{\nu}}^{I\alpha}) (\tilde{L}_i^+ (\partial^\mu - \overleftarrow{\partial}^\mu) \tilde{\nu}^\alpha). \quad (15)$$

From the interactions of gauge and matter multiplets  $ig\sqrt{2}T_{ij}^a(\lambda^a\psi_j A_i^* - \bar{\lambda}^a\bar{\psi}_i A_j)$ , the  $l$ - $\chi_L^0$ - $\tilde{L}$  coupling is deduced here:

$$\mathcal{L}_{l\chi_L^0\tilde{L}} = \sqrt{2}g_L \bar{\chi}_{Lj}^0 \left( Z_{N_L}^{1j} Z_{\tilde{L}}^{Ii} P_L - Z_{N_L}^{1j*} Z_{\tilde{L}}^{(I+3)i} P_R \right) l^I \tilde{L}_i^+ + \text{h.c.} \quad (16)$$

The  $\nu$ - $\chi_L^0$ - $\tilde{\nu}$  coupling is

$$\begin{aligned} \mathcal{L}_{\nu\chi_L^0\tilde{\nu}} = & \left[ \sqrt{2}g_L Z_{N_L}^{1i} Z_{\tilde{\nu}}^{I\alpha} Z_{\tilde{\nu}}^{Jj*} \delta^{IJ} \right. \\ & - (Z_{N_L}^{3i} (\lambda_{N^c}^{IJ} + \lambda_{N^c}^{JI}) + \sqrt{2}g_L Z_{N_L}^{1i} \delta^{IJ}) \\ & \left. \times Z_{\tilde{\nu}}^{(I+3)\alpha} Z_{\tilde{\nu}}^{(J+3)j*} \right] \bar{\chi}_{L_i}^0 P_L \nu^\alpha \tilde{\nu}^{j*} + \text{h.c.} \quad (17) \end{aligned}$$

We also obtain the  $\chi^\pm$ - $l$ - $\tilde{\nu}$  coupling and the  $\chi^\pm$ - $\tilde{L}$ - $\nu$  coupling:

$$\begin{aligned} \mathcal{L}_{\chi^\pm l \tilde{\nu}} = & - \sum_{I,J=1}^3 \sum_{\alpha=1}^6 \bar{\chi}_j^\pm \left( Y_l^{IJ} Z_{\tilde{\nu}}^{2j*} (Z_{\tilde{\nu}}^{I\alpha})^* P_R \right. \\ & \left. + \left[ \frac{e}{s_W} Z_{\tilde{\nu}}^{1j} (Z_{\tilde{\nu}}^{I\alpha})^* + Y_l^{IJ} Z_{\tilde{\nu}}^{2j} (Z_{\tilde{\nu}}^{(I+3)\alpha})^* \right] P_L \right) l^J \tilde{\nu}^{\alpha*} \\ & + \text{h.c.} \end{aligned}$$

$$\begin{aligned} \mathcal{L}_{\chi^\pm \tilde{L} \nu} = & - \sum_{I,J=1}^3 \sum_{i=1}^2 \sum_{j,\alpha=1}^6 \bar{\chi}_i^\pm \left( Y_\nu^{IJ} Z_{\tilde{L}}^{2i*} Z_{\tilde{\nu}}^{Ij} Z_{\tilde{\nu}}^{(J+3)\alpha*} P_R \right. \\ & \left. + \left[ \frac{e}{s_W} Z_{\tilde{L}}^{1i} Z_{\tilde{L}}^{Ij} + Y_l^{IJ} Z_{\tilde{L}}^{2i} Z_{\tilde{L}}^{(I+3)j} \right] Z_{\tilde{\nu}}^{J\alpha} P_L \right) \nu^\alpha \tilde{L}_j^+ \\ & + \text{h.c.} \quad (18) \end{aligned}$$

The  $\chi^0$ - $\tilde{\nu}$ - $\nu$  coupling in the BL MSSM becomes

$$\begin{aligned} \mathcal{L}_{\chi^0\tilde{\nu}\nu} = & \left[ Z_{\tilde{\nu}}^{I\alpha} Z_{\tilde{\nu}}^{Jj*} \frac{e}{\sqrt{2}s_W c_W} (Z_{N^c}^{1i} s_W - Z_{N^c}^{2i} c_W) \right. \\ & \left. + \frac{Y_\nu^{IJ}}{\sqrt{2}} Z_{N^c}^{4i} (Z_{\tilde{\nu}}^{I\alpha} Z_{\tilde{\nu}}^{(J+3)j*} + Z_{\tilde{\nu}}^{(I+3)\alpha} Z_{\tilde{\nu}}^{Jj*}) \right] \\ & \times \bar{\chi}_i^0 P_L \nu^\alpha \tilde{\nu}^{j*} + \text{h.c.} \quad (19) \end{aligned}$$

All the other couplings used are consistent with the MSSM.

## 5 Formulae

### 5.1 Observables

The observable  $R_{D^{(*)}}$  is defined as

$$R_{D^{(*)}} = \frac{\mathcal{B}_\tau^{D^{(*)}}}{\mathcal{B}_l^{D^{(*)}}} = \frac{\mathcal{B}(\bar{B} \rightarrow D^{(*)} \tau \bar{\nu}_\tau)}{\mathcal{B}(\bar{B} \rightarrow D^{(*)} l \bar{\nu}_l)}. \quad (20)$$

$\mathcal{B}_\ell^{D^{(*)}}$ , the branching fraction, is given by [4]:

$$\mathcal{B}_\ell^{D^{(*)}} = \int \mathcal{N} |p_{D^{(*)}}| (2a_\ell^{D^{(*)}} + \frac{2}{3}c_\ell^{D^{(*)}}) dq^2, \quad (21)$$

where  $l = e$  or  $\mu$ , and  $\ell$  denotes any lepton ( $e, \mu$  or  $\tau$ ).  $q^2$  is the invariant mass squared of the lepton-neutrino system, whose integral interval is  $[m_\ell^2, (M_B - M_{D^{(*)}})^2]$ .  $\mathcal{N}$ , the normalisation factor, is given by

$$\mathcal{N} = \frac{\tau_B G_F^2 |V_{cb}|^2 q^2}{256\pi^3 M_B^2} \left(1 - \frac{m_\ell^2}{q^2}\right)^2. \quad (22)$$

Here  $\tau_B$  is the lifetime of the  $B$ -meson.  $G_F = \sqrt{2}e^2/8m_W^2 s_W^2$  is the Fermi coupling constant.  $|p_{D^{(*)}}|$ , the absolute value of the  $D^{(*)}$ -meson momentum, is given by

$$|p_{D^{(*)}}| = \frac{\sqrt{(M_B^2)^2 + (M_{D^{(*)}}^2)^2 + (q^2)^2 - 2(M_B^2 M_{D^{(*)}}^2 + M_{D^{(*)}}^2 q^2 + q^2 M_B^2)}}{2M_B}. \quad (23)$$

The expressions for  $a_\ell^D$  and  $c_\ell^D$  are [4]:

$$\begin{aligned} a_\ell^D = & 8 \left\{ \frac{M_B^2 |p_D|^2}{q^2} (|\mathcal{C}_{VL}^\ell|^2 + |\mathcal{C}_{VR}^\ell|^2) \mathbf{F}_+^2 + \frac{(M_B^2 - M_D^2)^2}{4(m_b - m_c)^2} (|\mathcal{C}_{SL}^\ell|^2 + |\mathcal{C}_{SR}^\ell|^2) \mathbf{F}_0^2 \right. \\ & + m_\ell \left[ \frac{(M_B^2 - M_D^2)^2}{2q^2 (m_b - m_c)} (\mathcal{R}(\mathcal{C}_{SL}^\ell \mathcal{C}_{VL}^{\ell*}) + \mathcal{R}(\mathcal{C}_{SR}^\ell \mathcal{C}_{VR}^{\ell*})) \mathbf{F}_0^2 + \frac{4M_B^2 |p_D|^2}{q^2 (M_B + M_D)} (\mathcal{R}(\mathcal{C}_{TL}^\ell \mathcal{C}_{VL}^{\ell*}) + \mathcal{R}(\mathcal{C}_{TR}^\ell \mathcal{C}_{VR}^{\ell*})) \mathbf{F}_+ \mathbf{F}_T \right] \\ & \left. + m_\ell^2 \left[ \frac{(M_B^2 - M_D^2)^2}{4q^4} (|\mathcal{C}_{VL}^\ell|^2 + |\mathcal{C}_{VR}^\ell|^2) \mathbf{F}_0^2 + \frac{4|p_D|^2 M_B^2}{q^2 (M_B + M_D)^2} (|\mathcal{C}_{TL}^\ell|^2 + |\mathcal{C}_{TR}^\ell|^2) \mathbf{F}_T^2 \right] \right\}, \quad (24) \end{aligned}$$

$$c_D^D = 8 \left\{ \frac{4M_B^2 |p_D|^2}{(M_B + M_D)^2} (|C_{TL}^\ell|^2 + |C_{TR}^\ell|^2) \mathbf{F}_T^2 - \frac{M_B^2 |p_D|^2}{q^2} (|C_{VL}^\ell|^2 + |C_{VR}^\ell|^2) \mathbf{F}_+^2 + m_\ell^2 \left[ \frac{|p_D|^2 M_B^2}{q^4} (|C_{VL}^\ell|^2 + |C_{VR}^\ell|^2) \mathbf{F}_+^2 - \frac{4|p_D|^2 M_B^2}{(M_B + M_D)^2 q^2} (|C_{TL}^\ell|^2 + |C_{TR}^\ell|^2) \mathbf{F}_T^2 \right] \right\}. \quad (25)$$

The full expressions for  $a_\ell^{D^*}$ ,  $c_\ell^{D^*}$  and all form factors ( $\mathbf{F}_T(q^2)$ ,  $\mathbf{F}_+(q^2)$  and  $\mathbf{F}_0(q^2)$ , etc) are given in Refs. [4, 47].

## 5.2 Effective Lagrangian

We use effective field theory to calculate the theoretical values. The effective Lagrangian for the  $b \rightarrow c\ell\bar{\nu}^\ell$  process is

$$\mathcal{L}_{\text{eff}}^{b \rightarrow c\ell\bar{\nu}^\ell} = \sqrt{2}G_F V_{cb} (C_{VL}^\ell \mathcal{O}_{VL}^\ell + C_{VR}^\ell \mathcal{O}_{VR}^\ell + C_{AL}^\ell \mathcal{O}_{AL}^\ell + C_{AR}^\ell \mathcal{O}_{AR}^\ell + C_{SL}^\ell \mathcal{O}_{SL}^\ell + C_{SR}^\ell \mathcal{O}_{SR}^\ell + C_{PL}^\ell \mathcal{O}_{PL}^\ell + C_{PR}^\ell \mathcal{O}_{PR}^\ell + C_{TL}^\ell \mathcal{O}_{TL}^\ell + C_{TR}^\ell \mathcal{O}_{TR}^\ell), \quad (26)$$

where  $V_{cb}=0.04$ , and the full set of operators is [48]:

$$\begin{aligned} \mathcal{O}_{VL}^\ell &= [\bar{c}\gamma^\mu b][\bar{\ell}\gamma_\mu P_L \nu^\ell], & \mathcal{O}_{VR}^\ell &= [\bar{c}\gamma^\mu b][\bar{\ell}\gamma_\mu P_R \nu^\ell], \\ \mathcal{O}_{AL}^\ell &= [\bar{c}\gamma^\mu \gamma_5 b][\bar{\ell}\gamma_\mu P_L \nu^\ell], & \mathcal{O}_{AR}^\ell &= [\bar{c}\gamma^\mu \gamma_5 b][\bar{\ell}\gamma_\mu P_R \nu^\ell], \\ \mathcal{O}_{SL}^\ell &= [\bar{c}b][\bar{\ell}P_L \nu^\ell], & \mathcal{O}_{SR}^\ell &= [\bar{c}b][\bar{\ell}P_R \nu^\ell], \\ \mathcal{O}_{PL}^\ell &= [\bar{c}\gamma_5 b][\bar{\ell}P_L \nu^\ell], & \mathcal{O}_{PR}^\ell &= [\bar{c}\gamma_5 b][\bar{\ell}P_R \nu^\ell], \\ \mathcal{O}_{TL}^\ell &= [\bar{c}\sigma^{\mu\nu} b][\bar{\ell}\sigma_{\mu\nu} P_L \nu^\ell], & \mathcal{O}_{TR}^\ell &= [\bar{c}\sigma^{\mu\nu} b][\bar{\ell}\sigma_{\mu\nu} P_R \nu^\ell]. \end{aligned} \quad (27)$$

In the SM,  $C_{VL}^\ell = -C_{AL}^\ell = 1$  and all the other WCs vanish. In the BLMSSM, we calculate all the WCs at one-loop level to obtain the theoretical values.

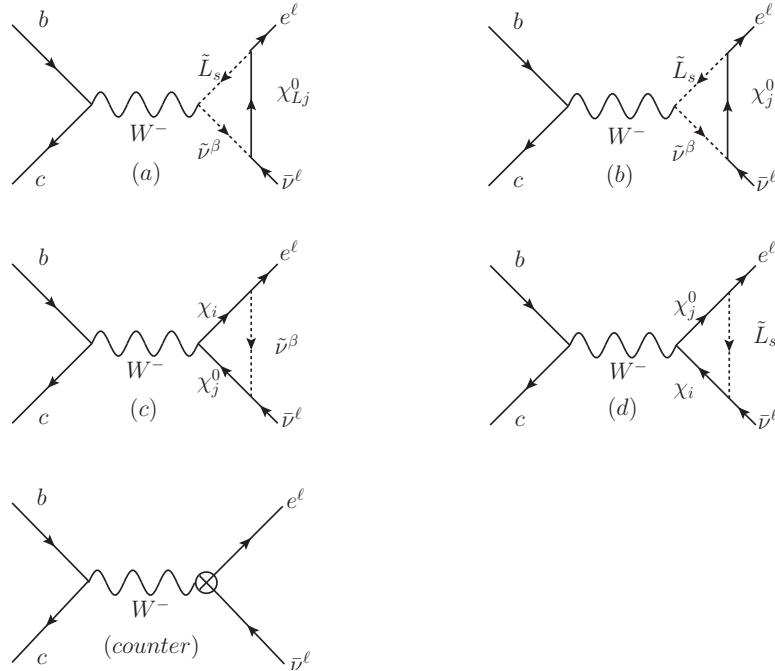


Fig. 1. The penguin-type Feynman diagrams that can correct  $R_{D^{(*)}}$  in the BLMSSM.

## 6 Feynman diagrams

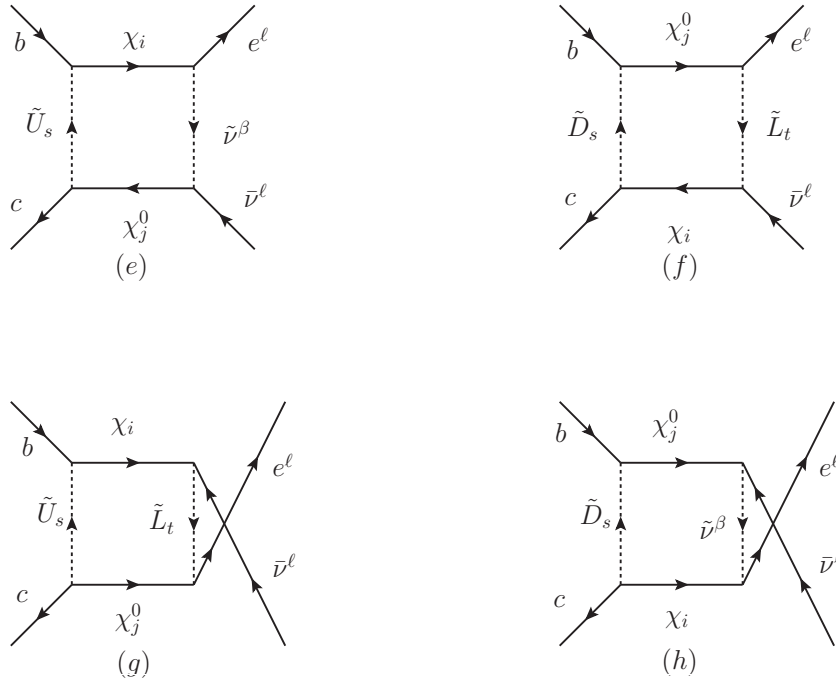
In the BLMSSM, the one-loop Feynman diagrams for the lepton sector that can correct the anomalies are shown in Fig. 1 and Fig. 2.

### 6.1 Penguin-type Feynman diagrams

#### 6.1.1 The WCs

The one-loop Feynman diagrams in Fig. 1(a),(b),(c) and (d) are all UV divergent. Focusing on Fig. 1(a), the three lepton-neutralinos  $\chi_L^0$  are new particles in the BLMSSM, and they play very important roles in this decay process. So taking Fig. 1(a) as an example, the non-zero WCs in Eq. (26) are given as follows:

$$\begin{aligned} C_{VL(a)}^\ell &= \left[ \sum_{\beta,s=1}^6 \sum_{j=1}^3 \frac{\mathcal{B}_1^{\ell s j} \mathcal{A}_2^{\beta \ell j} \mathcal{A}_3^{\beta s} \mathcal{A}_4}{m_W^2} \frac{1}{64\pi^2} (\Delta_{UV} + 1 - F_{21}(x_{\chi_{Lj}^0}, x_{\tilde{L}_s}, x_{\tilde{\nu}^\ell})) \right] / (\sqrt{2}G_F V_{cb}) \\ &= \frac{g_L^2}{16\pi^2} \Delta_{UV} + \text{finite terms}, \\ C_{AL(a)}^\ell &= -C_{VL(a)}^\ell. \end{aligned} \quad (28)$$


 Fig. 2. The box-type Feynman diagrams that can correct  $R_{D^{(*)}}$  in the BLMSSM.

Here, we use the unitary characteristics of the rotation matrices. In Eq. (28),

$$\begin{aligned} \mathcal{B}_1^{\ell sj} &= \sqrt{2}g_L Z_{N_L}^{1j*} Z_L^{\ell s*}, \\ \mathcal{A}_2^{\beta \ell j} &= \sum_{I=1}^3 \left( \sqrt{2}g_L Z_{N_L}^{1j} Z_\nu^{I\ell} Z_\nu^{I\beta} - (2\lambda_{N_c}^{II} Z_{N_L}^{3j} + \sqrt{2}g_L Z_{N_L}^{1j}) \right. \\ &\quad \left. \times Z_\nu^{(I+3)\ell} Z_\nu^{(I+3)\beta*} \right), \\ \mathcal{A}_3^{\beta s} &= -\sum_{I=1}^3 \left( \frac{e}{\sqrt{2}s_W} Z_\nu^{I\beta} Z_L^{Is} \right), \quad \mathcal{A}_4 = -\frac{e}{\sqrt{2}s_W} V_{cb}. \end{aligned} \quad (29)$$

$\Delta_{UV} = 1/\epsilon + \ln(4\pi\kappa^2/\Lambda_{\text{NP}}^2) - \gamma_E$ ,  $\frac{1}{\epsilon}$  is an infinite term, the mass scale  $\kappa$  is introduced in the dimensional regularization,  $\Lambda_{\text{NP}}$  is the NP scale, and  $\gamma_E$  is the Euler-Mascheroni constant.  $x_i$  represents  $\frac{m_i^2}{\Lambda_{\text{NP}}^2}$ , and the concrete form of formula  $F_{21}(x_1, x_2, x_3)$  is given in the Appendix.

We can see that the infinite terms of the WCs of Fig. 1(a) are  $\mathcal{C}_{VL(a)}^{\ell(IF)} = \frac{g_L^2}{16\pi^2} \Delta_{UV}$  and  $\mathcal{C}_{AL(a)}^{\ell(IF)} = -\mathcal{C}_{VL(a)}^{\ell(IF)}$ . Similarly, the infinite terms of the WCs of the following three diagrams (Fig. 1(b), (c) and (d)) are given as follows:

$$\begin{aligned} \mathcal{C}_{VL(b)}^{\ell(IF)} &= \frac{e^2}{64\pi^2 s_W^2 c_W^2} (1 - 2c_W^2) \Delta_{UV}, & \mathcal{C}_{AL(b)}^{\ell(IF)} &= -\mathcal{C}_{VL(b)}^{\ell(IF)}, \\ \mathcal{C}_{VL(c)}^{\ell(IF)} &= \frac{e^2}{32\pi^2 s_W^2} \Delta_{UV}, & \mathcal{C}_{AL(c)}^{\ell(IF)} &= -\mathcal{C}_{VL(c)}^{\ell(IF)}, \\ \mathcal{C}_{VL(d)}^{\ell(IF)} &= \left( \frac{e^2}{32\pi^2 s_W^2} + \frac{(Y_L^\ell)^2}{32\pi^2} \right) \Delta_{UV}, & \mathcal{C}_{AL(d)}^{\ell(IF)} &= -\mathcal{C}_{VL(d)}^{\ell(IF)}. \end{aligned} \quad (30)$$

Now we should deal with the UV divergences by renormalization procedures.

### 6.1.2 The counter term in the on-shell scheme

Considering the final state lepton and neutrino are both real particles, we use the on-shell scheme to eliminate the infinite terms. To obtain finite results, the contributions from the counter terms for the vertex  $\bar{l}^I \nu^I W^-$  are necessary. The counter term formula for the vertex  $\bar{l}^I \nu^I W^-$  is:

$$\begin{aligned} \delta V_{\bar{l}^I \nu^I W^-}^\mu \text{ (OS)} &= \frac{-ie}{2\sqrt{2}s_W} \left( \frac{\delta m_Z^2}{m_Z^2} - \frac{\delta m_Z^2 - \delta m_W^2}{m_Z^2 - m_W^2} + 2\delta e + \delta Z_L^{II} \right. \\ &\quad \left. + \delta Z_L^{\nu I} + \delta Z_{WW} \right) \gamma^\mu P_L, \end{aligned} \quad (31)$$

Following the method in Refs. [49–51], we obtain the needed renormalization constants in the BLMSSM.

We calculate the Z boson self-energy diagram (loop particles are sneutrinos or sleptons) and get the renormalization constant  $\delta m_Z^2$ :

$$\begin{aligned} \frac{\delta m_Z^2}{m_Z^2} &= \left[ \frac{e^2}{32\pi^2 s_W^2 c_W^2} (1 - 2s_W^2)^2 + \frac{e^2}{16\pi^2 c_W^2} \right] \Delta_{UV} \\ &\quad - \frac{e^2}{s_W^2 c_W^2} \left\{ \frac{1}{4} \sum_{j=1}^6 F_1(x_{\tilde{\nu}_j}, x_{\tilde{\nu}_j}) \right. \\ &\quad \left. + \sum_{\alpha, \beta=1}^6 |(\mathcal{G})_{\alpha\beta}|^2 F_1(x_{\tilde{L}_\alpha}, x_{\tilde{L}_\beta}) \right\}. \end{aligned} \quad (32)$$

Through calculating the W boson self-energy diagram (with sneutrinos and sleptons in the loop), we can obtain:

$$\begin{aligned}\frac{\delta m_W^2}{m_Z^2} &= \frac{e^2 c_W^2}{32\pi^2 s_W^2} \Delta_{UV} - \frac{e^2 c_W^2}{2s_W^2} \sum_{i=1}^6 \sum_{\alpha=1}^6 |(\eta)_{i\alpha}|^2 F_1(x_{\tilde{\nu}_\alpha}, x_{\tilde{L}_i}), \\ \delta Z_{WW} &= -\frac{e^2}{32\pi^2 s_W^2} \Delta_{UV} + \frac{e^2}{2s_W^2} \sum_{i=1}^6 \sum_{\alpha=1}^6 |(\eta)_{i\alpha}|^2 F_1(x_{\tilde{\nu}_\alpha}, x_{\tilde{L}_i}).\end{aligned}\quad (33)$$

The renormalization constant of charge is obtained from virtual sleptons:

$$\delta e = \frac{e^2}{16\pi^2} \Delta_{UV} - \frac{1}{2} e^2 \sum_{i=1}^6 F_1(x_{\tilde{L}_i}, x_{\tilde{L}_i}). \quad (34)$$

In the same way, we give the renormalization constants  $\delta Z_L^{\nu I}$  and  $\delta Z_L^{l I}$  for neutrinos and leptons respectively:

$$\begin{aligned}\delta Z_L^{\nu I} &= \frac{-e^2}{32\pi^2 s_W^2} \left( \frac{1}{2c_W^2} + 1 + \left( \frac{s_W Y_l^I}{e} \right)^2 + \left( \frac{\sqrt{2} s_W g_L}{e} \right)^2 \right) \Delta_{UV} - \frac{e^2}{2s_W^2 c_W^2} \sum_{i=1}^4 \sum_{\alpha=1}^6 |(\zeta^I)_{\alpha i}|^2 F_2(x_{\tilde{\nu}_\alpha}, x_{\chi_i^0}) \\ &\quad - \frac{e^2}{s_W^2} \sum_{i=1}^2 \sum_{\alpha=1}^6 |(\mathcal{P}^I)_{\alpha i}|^2 F_2(x_{\tilde{L}_\alpha}, x_{\chi_i^-}) - \frac{e^2}{2s_W^2 c_W^2} \sum_{i=1}^3 \sum_{\alpha=1}^6 |(\zeta'^I)_{\alpha i}|^2 F_2(x_{\tilde{\nu}_\alpha}, x_{\chi_{L_i}^0}), \\ \delta Z_L^{l I} &= \frac{-e^2}{32\pi^2 s_W^2} \left( \frac{1}{2c_W^2} + 1 + \left( \frac{s_W Y_l^I}{e} \right)^2 + \left( \frac{\sqrt{2} s_W g_L}{e} \right)^2 \right) \Delta_{UV} \\ &\quad - \frac{e^2}{s_W^2} \sum_{\alpha=1}^6 \sum_{i=1}^2 \left\{ |(\mathcal{B}_i)^{I\alpha}|^2 F_2 + x_{eI} \left[ |(\mathcal{B}_i)^{I\alpha}|^2 + |(\mathcal{A}_i)^{I\alpha}|^2 + 2\text{Re}[(\mathcal{A}_i^\dagger)^{I\alpha} (\mathcal{B}_i)^{I\alpha}] \right] F_3 \right\} (x_{\tilde{\nu}_\alpha}, x_{\chi_i^-}) \\ &\quad - e^2 \sum_{j=1}^4 \sum_{i=1}^6 \left\{ x_{eI} \left[ \frac{|(\mathcal{D}^I)_{ij}|^2}{2s_W^2} + \frac{\sqrt{2}}{s_W} \text{Re}[(\mathcal{C}^I)_{ij}^\dagger (\mathcal{D}^I)_{ij}] + |(\mathcal{C}^I)_{ij}|^2 \right] F_3 + \frac{1}{2s_W^2} |(\mathcal{D}^I)_{ij}|^2 F_2 \right\} (x_{\tilde{L}_i}, x_{\chi_j^0}) \\ &\quad - e^2 \sum_{j=1}^3 \sum_{i=1}^6 \left\{ x_{eI} \left[ \frac{|(\mathcal{D}'^I)_{ij}|^2}{2s_W^2} + \frac{\sqrt{2}}{s_W} \text{Re}[(\mathcal{C}'^I)_{ij}^\dagger (\mathcal{D}'^I)_{ij}] + |(\mathcal{C}'^I)_{ij}|^2 \right] F_3 + \frac{1}{2s_W^2} |(\mathcal{D}'^I)_{ij}|^2 F_2 \right\} (x_{\tilde{L}_i}, x_{\chi_{L_j}^0}),\end{aligned}\quad (35)$$

where the vertex couplings are given by

$$\begin{aligned}(\mathcal{A}_i)^{I\alpha} &= \frac{Y_l^I s_W}{e} Z_-^{2i*} Z_{\tilde{\nu}}^{I\alpha*}, \quad (\mathcal{B}_i)^{I\alpha} = Z_+^{1i} Z_{\tilde{\nu}}^{I\alpha*}, \quad (\eta)_{i\alpha} = Z_{\tilde{\nu}}^{J\alpha} Z_{\tilde{L}}^{Ji}, \\ (\mathcal{P}^I)_{\alpha i} &= \frac{-Y_l^J s_W}{e} Z_{\tilde{\nu}}^{JI} Z_{\tilde{L}}^{(J+3)\alpha*} Z_-^{2i*} - Z_{\tilde{\nu}}^{JI} Z_{\tilde{L}}^{J\alpha*} Z_-^{1i*}, \\ (\zeta^I)_{\alpha i} &= Z_{\tilde{\nu}}^{J\alpha*} Z_{\tilde{\nu}}^{JI} (Z_N^{1i} s_W - Z_N^{2i} c_W), \quad (\mathcal{C}^I)_{ij} = \frac{-\sqrt{2}}{c_W} Z_{\tilde{L}}^{(I+3)i} Z_N^{1j*} + \frac{Y_l^I}{e} Z_{\tilde{L}}^{Ii} Z_N^{3j*}, \\ (\mathcal{D}^I)_{ij} &= \frac{Z_{\tilde{L}}^{Ii}}{c_W} (Z_N^{1j} s_W + Z_N^{2j} c_W) + \frac{\sqrt{2} s_W Y_l^I}{e} Z_{\tilde{L}}^{(I+3)i} Z_N^{3j}, \\ (\mathcal{G})_{\alpha\beta} &= \frac{1}{2} Z_{\tilde{L}}^{J\alpha} Z_{\tilde{L}}^{J\beta*} - s_W^2 \delta^{\alpha\beta}, \quad (\mathcal{C}'^I)_{ij} = \frac{-\sqrt{2} g_L}{e} Z_{NL}^{1j*} Z_{\tilde{L}}^{(I+3)i}, \quad (\mathcal{D}'^I)_{ij} = \frac{2g_L s_W}{e} Z_{NL}^{1j} Z_{\tilde{L}}^{Ii}, \\ (\zeta'^I)_{\alpha i} &= \frac{\sqrt{2} s_W c_W}{e} (\sqrt{2} g_L Z_{NL}^{1i} Z_{\tilde{\nu}}^{JI} Z_{\tilde{\nu}}^{J\alpha*} - [2\lambda_{Nc}^{JJ} Z_{NL}^{3i} + \sqrt{2} g_L Z_{NL}^{1i}] Z_{\tilde{\nu}}^{(J+3)I} Z_{\tilde{\nu}}^{(J+3)\alpha*}).\end{aligned}\quad (36)$$

The functions  $F_1, F_2$ , and  $F_3$  are as follows:

$$\begin{aligned}F_1(x_1, x_2) &= \frac{1}{288\pi^2 (x_1 - x_2)^3} [6(x_1 - 3x_2)x_1^2 \ln x_1 + 6(3x_1 - x_2)x_2^2 \ln x_2 - (x_1 - x_2)(5x_1^2 - 22x_1 x_2 + 5x_2^2)], \\ F_2(x_1, x_2) &= \frac{(2x_2 - x_1)(x_2 - x_1 + x_1 \ln x_1) - x_2^2 \ln x_2}{32\pi^2 (x_1 - x_2)^2}, \\ F_3(x_1, x_2) &= \frac{x_1^2 + 2x_1 x_2 (\ln x_2 - \ln x_1) - x_2^2}{32\pi^2 (x_1 - x_2)^3}.\end{aligned}\quad (37)$$

If  $x_1 = x_2$ , they simplify to

$$F_1(x_1, x_2) = \frac{\ln x_1}{48\pi^2}, \quad F_2(x_1, x_2) = -\frac{\ln x_1}{32\pi^2} + \frac{1}{64\pi^2}, \quad F_3(x_1, x_2) = \frac{1}{96\pi^2 x_1}. \quad (38)$$

Now, the WCs of Fig. 1(counter) read:

$$\begin{aligned} \mathcal{C}_{VL(\text{counter})}^\ell &= \frac{1}{2} \left( \frac{\delta m_Z^2}{m_Z^2} - \frac{\delta m_Z^2 - \delta m_W^2}{m_Z^2 - m_W^2} + 2\delta e + \delta Z_L^\ell + \delta Z_L^{\nu\ell} + \delta Z_{WW} \right), \\ \mathcal{C}_{AL(\text{counter})}^\ell &= -\mathcal{C}_{VL(\text{counter})}^\ell. \end{aligned} \quad (39)$$

The corresponding  $\mathcal{C}_{VL(\text{counter})}^{\ell(IF)}$  and  $\mathcal{C}_{AL(\text{counter})}^{\ell(IF)}$  are:

$$\begin{aligned} \mathcal{C}_{VL(\text{counter})}^{\ell(IF)} &= \frac{1}{2} \left\{ \left[ \frac{e^2}{32\pi^2 s_W^2 c_W^2} (1 - 2s_W^2)^2 + \frac{e^2}{16\pi^2 c_W^2} \right] \Delta_{UV} \right. \\ &\quad - \left[ \left( \frac{e^2}{32\pi^2 s_W^2 c_W^2} (1 - 2s_W^2)^2 + \frac{e^2}{16\pi^2 c_W^2} \right) \Delta_{UV} - \frac{e^2 c_W^2}{32\pi^2 s_W^2} \Delta_{UV} \right] \frac{m_Z^2}{m_Z^2 - m_W^2} \\ &\quad \left. + \frac{e^2}{8\pi^2} \Delta_{UV} - \frac{e^2}{32\pi^2 s_W^2} \Delta_{UV} + \frac{-e^2}{16\pi^2 s_W^2} \left[ \frac{1}{2c_W^2} + 1 + \left( \frac{s_W Y_l^\ell}{e} \right)^2 + \left( \frac{\sqrt{2} s_W g_L}{e} \right)^2 \right] \Delta_{UV} \right\}, \\ \mathcal{C}_{AL(\text{counter})}^{\ell(IF)} &= -\mathcal{C}_{VL(\text{counter})}^{\ell(IF)}. \end{aligned} \quad (40)$$

It is easy to test that the infinite terms in the sum of Fig. 1(a),(b),(c),(d) and (counter) vanish:  $\mathcal{C}_{VL}^{\ell(IF)} = \mathcal{C}_{VL(a)}^{\ell(IF)} + \mathcal{C}_{VL(b)}^{\ell(IF)} + \mathcal{C}_{VL(c)}^{\ell(IF)} + \mathcal{C}_{VL(d)}^{\ell(IF)} + \mathcal{C}_{VL(\text{counter})}^{\ell(IF)} = 0$ , similarly,  $\mathcal{C}_{AL}^{\ell(IF)} = 0$ . Therefore, the divergences are completely eliminated. Note that the infinite terms in the sum of Fig. 1(a), (b), (c) and (d) can be eliminated by the counter terms. However, a single diagram in Fig. 1(b), (c), (d), such as Fig. 1(b), cannot be counteracted individually in the on-shell scheme.

## 6.2 Box-type Feynman diagrams

Taking Fig. 2(e) as an example, the corresponding WCs are given as follows:

$$\begin{aligned} \mathcal{C}_{VL(e)}^\ell &= \sum_{\beta, s=1}^6 \sum_{i=1}^2 \sum_{j=1}^4 \left[ \frac{\mathcal{B}_1^{\beta li} \mathcal{B}_2^{is} \mathcal{A}_3^{sj} \mathcal{A}_4^{\beta lj} m_{\chi_j^0} m_{\chi_i}}{\Lambda_{\text{NP}}^4} \frac{1}{64\pi^2} F_{11}(x_{\bar{\nu}\beta}, x_{\chi_j^0}, x_{\tilde{U}_s}, x_{\chi_i}) \right. \\ &\quad \left. - \frac{\mathcal{B}_1^{\beta li} \mathcal{A}_2^{is} \mathcal{B}_3^{sj} \mathcal{A}_4^{\beta lj}}{\Lambda_{\text{NP}}^2} \frac{1}{128\pi^2} F_{21}(x_{\bar{\nu}\beta}, x_{\chi_j^0}, x_{\tilde{U}_s}, x_{\chi_i}) \right] / (\sqrt{2} G_F V_{cb}), \end{aligned} \quad (41)$$

$$\begin{aligned} \mathcal{C}_{AL(e)}^\ell &= \sum_{\beta, s=1}^6 \sum_{i=1}^2 \sum_{j=1}^4 \left[ \frac{\mathcal{B}_1^{\beta li} \mathcal{B}_2^{is} \mathcal{A}_3^{sj} \mathcal{A}_4^{\beta lj} m_{\chi_j^0} m_{\chi_i}}{\Lambda_{\text{NP}}^4} \frac{1}{64\pi^2} F_{11}(x_{\bar{\nu}\beta}, x_{\chi_j^0}, x_{\tilde{U}_s}, x_{\chi_i}) \right. \\ &\quad \left. + \frac{\mathcal{B}_1^{\beta li} \mathcal{A}_2^{is} \mathcal{B}_3^{sj} \mathcal{A}_4^{\beta lj}}{\Lambda_{\text{NP}}^2} \frac{1}{128\pi^2} F_{21}(x_{\bar{\nu}\beta}, x_{\chi_j^0}, x_{\tilde{U}_s}, x_{\chi_i}) \right] / (\sqrt{2} G_F V_{cb}), \end{aligned} \quad (42)$$

$$\begin{aligned} \mathcal{C}_{SL(e)}^\ell &= \sum_{\beta, s=1}^6 \sum_{i=1}^2 \sum_{j=1}^4 \left[ \frac{\mathcal{A}_1^{\beta li} \mathcal{A}_2^{is} \mathcal{A}_3^{sj} \mathcal{A}_4^{\beta lj} m_{\chi_j^0} m_{\chi_i}}{\Lambda_{\text{NP}}^4} \frac{1}{64\pi^2} F_{11}(x_{\bar{\nu}\beta}, x_{\chi_j^0}, x_{\tilde{U}_s}, x_{\chi_i}) \right. \\ &\quad \left. + \frac{\mathcal{A}_1^{\beta li} \mathcal{B}_2^{is} \mathcal{B}_3^{sj} \mathcal{A}_4^{\beta lj}}{\Lambda_{\text{NP}}^2} \frac{1}{64\pi^2} F_{21}(x_{\bar{\nu}\beta}, x_{\chi_j^0}, x_{\tilde{U}_s}, x_{\chi_i}) \right] / (\sqrt{2} G_F V_{cb}), \end{aligned} \quad (43)$$

$$\begin{aligned} \mathcal{C}_{TL(e)}^\ell &= \left[ \sum_{\beta, s=1}^6 \sum_{i=1}^2 \sum_{j=1}^4 \frac{\mathcal{A}_1^{\beta li} \mathcal{A}_2^{is} \mathcal{A}_3^{sj} \mathcal{A}_4^{\beta lj} m_{\chi_j^0} m_{\chi_i}}{\Lambda_{\text{NP}}^4} \frac{1}{128\pi^2} F_{11}(x_{\bar{\nu}\beta}, x_{\chi_j^0}, x_{\tilde{U}_s}, x_{\chi_i}) \right] \\ &\quad / (\sqrt{2} G_F V_{cb}), \end{aligned} \quad (44)$$

$$\begin{aligned} \mathcal{C}_{PL(e)}^\ell &= \sum_{\beta, s=1}^6 \sum_{i=1}^2 \sum_{j=1}^4 \left[ -\frac{(\mathcal{A}_1^{\beta li} \mathcal{A}_2^{is} - \mathcal{B}_1^{\beta li} \mathcal{B}_2^{is}) \mathcal{A}_3^{sj} \mathcal{A}_4^{\beta lj} m_{\chi_j^0} m_{\chi_i}}{\Lambda_{\text{NP}}^4} \frac{1}{128\pi^2} F_{11}(x_{\bar{\nu}\beta}, x_{\chi_j^0}, x_{\tilde{U}_s}, x_{\chi_i}) \right. \\ &\quad \left. + \frac{\mathcal{A}_1^{\beta li} \mathcal{B}_2^{is} \mathcal{B}_3^{sj} \mathcal{A}_4^{\beta lj}}{\Lambda_{\text{NP}}^2} \frac{1}{64\pi^2} F_{21}(x_{\bar{\nu}\beta}, x_{\chi_j^0}, x_{\tilde{U}_s}, x_{\chi_i}) \right] / (\sqrt{2} G_F V_{cb}), \end{aligned} \quad (45)$$



$$C_{PR(e)}^{\ell} = \left[ \sum_{\beta,s=1}^6 \sum_{i=1}^2 \sum_{j=1}^4 - \frac{(\mathcal{A}_1^{\beta\ell i} \mathcal{A}_2^{is} + \mathcal{B}_1^{\beta\ell i} \mathcal{B}_2^{is}) \mathcal{A}_3^{sj} \mathcal{A}_4^{\beta\ell j} m_{\chi_j^0} m_{\chi_i}}{\Lambda_{\text{NP}}^4} \frac{1}{128\pi^2} F_{11}(x_{\tilde{\nu}\beta}, x_{\chi_j^0}, x_{\tilde{U}_s}, x_{\chi_i}) \right] / (\sqrt{2} G_F V_{cb}), \quad (46)$$

and all the other WCs in Eq. (26) vanish. In Eqs. (41-46),

$$\begin{aligned} \mathcal{A}_1^{\beta\ell i} &= -Y_l^{\ell} Z_{-}^{2i} Z_{\tilde{\nu}}^{\ell\beta}, \quad \mathcal{A}_2^{is} = \sum_{I=1}^3 \left( \frac{-e}{s_W} Z_{\tilde{U}}^{Is*} Z_{+}^{1i} + Y_u^I Z_{\tilde{U}}^{(I+3)*} Z_{+}^{2i} \right) V_{I3}, \\ \mathcal{A}_3^{sj} &= \frac{2\sqrt{2}e}{3c_W} Z_{\tilde{U}}^{5s} Z_N^{1j} - Y_u^2 Z_{\tilde{U}}^{2s} Z_N^{4j}, \\ \mathcal{A}_4^{\beta\ell j} &= \sum_{I=1}^3 \left\{ Z_{\tilde{\nu}}^{I\beta*} Z_{\nu}^{I\ell} \frac{e}{\sqrt{2}s_W c_W} (Z_N^{1j} s_W - Z_N^{2j} c_W) + \sum_{J=1}^3 \left( \frac{Y_{\nu}^{IJ}}{\sqrt{2}} Z_N^{4j} (Z_{\nu}^{I\ell} Z_{\tilde{\nu}}^{(J+3)\beta*} + Z_{\nu}^{(I+3)\ell} Z_{\tilde{\nu}}^{J\beta*}) \right) \right\}, \\ \mathcal{B}_1^{\beta\ell i} &= -\frac{e}{s_W} Z_{+}^{1i*} Z_{\tilde{\nu}}^{\ell\beta} - \sum_{I=1}^3 (Y_{\nu}^{\ell I} Z_{+}^{2i*} Z_{\tilde{\nu}}^{(I+3)\beta}), \quad \mathcal{B}_2^{is} = -\sum_{I=1}^3 (Y_d^3 Z_{\tilde{U}}^{Is*} Z_{-}^{2i*}) V_{I3}, \\ \mathcal{B}_3^{sj} &= -\frac{e}{\sqrt{2}s_W c_W} Z_{\tilde{U}}^{2s} \left( \frac{1}{3} Z_N^{1j*} s_W + Z_N^{2j*} c_W \right) - Y_u^2 Z_{\tilde{U}}^{5s} Z_N^{4j*}. \end{aligned} \quad (47)$$

The formulae  $F_{11}(x_1, x_2, x_3, x_4)$  and  $F_{21}(x_1, x_2, x_3, x_4)$  are given in the Appendix.

## 7 Numerical results

For the numerical discussion, the parameters used are:

$m_1=400$  GeV,  $M_L=2000$  GeV,  $\mu_L=1600$  GeV,  $\tan\beta_L=0.1$ ,  $v_L=1260$  GeV,  $\lambda_{Nc}=1$ ,  $\Lambda_{\text{NP}}=1000$  GeV,  $(m_Q^2)_{ii}=(m_U^2)_{ii}=(m_D^2)_{ii}=(m_{Nc}^2)_{ii}=3\times 10^6$  GeV<sup>2</sup>,  $(A_l)_{ii}=(A'_l)_{ii}=300$  GeV,  $(A_N)_{ii}=(A_{Nc})_{ii}=500$  GeV, and  $(A_u)_{ii}=(A_d)_{ii}=(A'_u)_{ii}=(A'_d)_{ii}=500$  GeV, where  $i=1\dots 3$ . If not otherwise noted, the non-diagonal elements of the parameters used should be zero. The Yukawa couplings of neutrinos  $Y_{\nu}^{IJ}$  are of the order of  $10^{-8}\sim 10^{-6}$ ; their effects are tiny and can be ignored.

At present, all supersymmetric mass bounds are model-dependent. Based on the PDG [52] data, we consider the limitations on masses of the charginos and neutralinos (the strongest limitations are 345 GeV). In our work, the masses of charginos  $m_{\chi^{\pm}} \simeq (1000\sim 2000)$  GeV and the masses of neutralinos  $m_{\chi^0} \simeq (400\sim 2000)$  GeV, all of which can satisfy the mass bounds. The limits for the sleptons are around 290 GeV  $\sim$  450 GeV [53], which can be satisfied easily. The masses of squarks in this paper are larger than 1000 GeV, so the limits for squarks are also satisfied. In other words, the parameters given above and the parameter space to be discussed below can all satisfy the mass bounds.

### 7.1 Effects of parameters $m_L^2$ (or $m_R^2$ ) on $R_{D^{(*)}}$

We now focus on the effects of parameters  $m_L^2$  (or  $m_R^2$ ) on  $R_{D^{(*)}}$ . First, we set the parameters as follows:  $\tan\beta=10$ ,  $m_2=\mu=1200$  GeV,  $g_L=0.1$ , and  $(m_L^2)_{33}=(m_R^2)_{33}=3\times 10^8$  GeV<sup>2</sup>.

To study the impacts of these parameters on  $R_{D^{(*)}}$ , we use the parameters  $(m_L^2)_{11}=(m_R^2)_{11}=(m_L^2)_{22}=(m_R^2)_{22}=3\times 10^{\xi}$  GeV<sup>2</sup>, where  $\xi$  is a variable. After calculation we obtain Fig. 3. Here, we used the central value of the SM prediction in our calculation. The left-hand diagram shows  $R_D$  and the right-hand diagram shows  $R_{D^*}$ .

We know the measurement of  $R_{D^{(*)}e}$  (which implies  $l=e$  in Eq. (20)) is approximately equal to that of  $R_{D^{(*)}\mu}$  ( $l=\mu$  in Eq. (20)). This is the reason why we set  $(m_L^2)_{11}=(m_R^2)_{11}=(m_L^2)_{22}=(m_R^2)_{22}$ . To solve the problem of  $R_{D^{(*)}}$ , we should violate lepton flavour symmetry for generations 1(2) and generation 3. Therefore, we suppose  $(m_L^2)_{33}=(m_R^2)_{33}\neq(m_L^2)_{11}$ .

It is easy to see from Fig. 3 that  $R_{D^{(*)}}$  decreases as  $\xi$  increases. Obviously, our results satisfy the decoupling rule. When the sleptons are very heavy, the BLMSSM results are very near the SM predictions. In fact, the SM predictions of  $R_{D^{(*)}}$  cannot explain the experimental values well, and our goal is to increase the theoretical values. From the numerical analysis, the following relational expression should be set up:  $(m_L^2)_{11}=(m_R^2)_{11}=(m_L^2)_{22}=(m_R^2)_{22}<(m_L^2)_{33}=(m_R^2)_{33}$ . We need to select a set of reasonable parameters, and finally choose:  $(m_L^2)_{11}=(m_R^2)_{11}=(m_L^2)_{22}=(m_R^2)_{22}=5.5\times 10^5$  GeV<sup>2</sup>, and  $(m_L^2)_{33}=(m_R^2)_{33}=3\times 10^8$  GeV<sup>2</sup>. Up to now, our theoretical values of  $R_{D^{(*)}}$  are only a little bigger than those of the SM, so we also need to study the effects of other parameters on  $R_{D^{(*)}}$ .

### 7.2 Effect of parameter $g_L$ on $R_{D^{(*)}}$

Based on the above analysis, we use the following parameters:

$$\begin{aligned} \tan\beta &= 10, \quad m_2 = \mu = 1200 \text{ GeV}, \\ (m_L^2)_{11} &= (m_R^2)_{11} = (m_L^2)_{22} = (m_R^2)_{22} = 5.5 \times 10^5 \text{ GeV}^2, \text{ and} \\ (m_L^2)_{33} &= (m_R^2)_{33} = 3 \times 10^8 \text{ GeV}^2. \end{aligned}$$

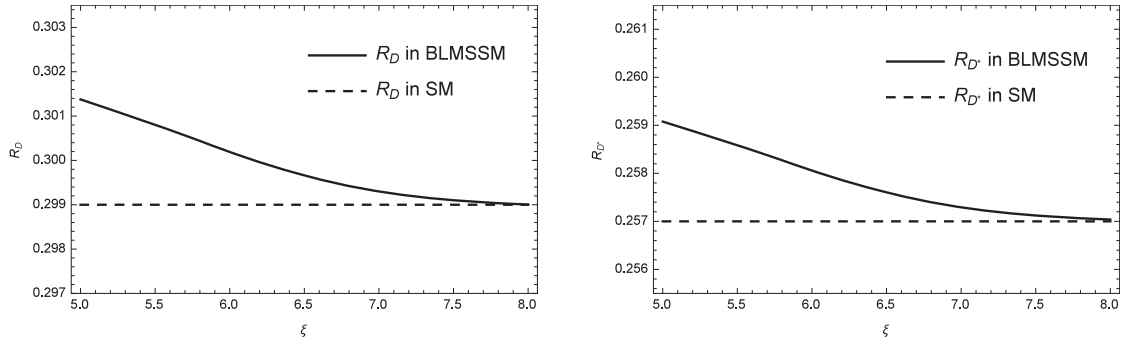


Fig. 3.  $R_D$  (left) and  $R_{D^*}$  (right) versus  $\xi$  with  $(m_{\tilde{L}}^2)_{11} = (m_{\tilde{R}}^2)_{11} = (m_{\tilde{L}}^2)_{22} = (m_{\tilde{R}}^2)_{22} = 3 \times 10^6 \text{ GeV}^2$ , and  $(m_{\tilde{L}}^2)_{33} = (m_{\tilde{R}}^2)_{33} = 3 \times 10^8 \text{ GeV}^2$ .

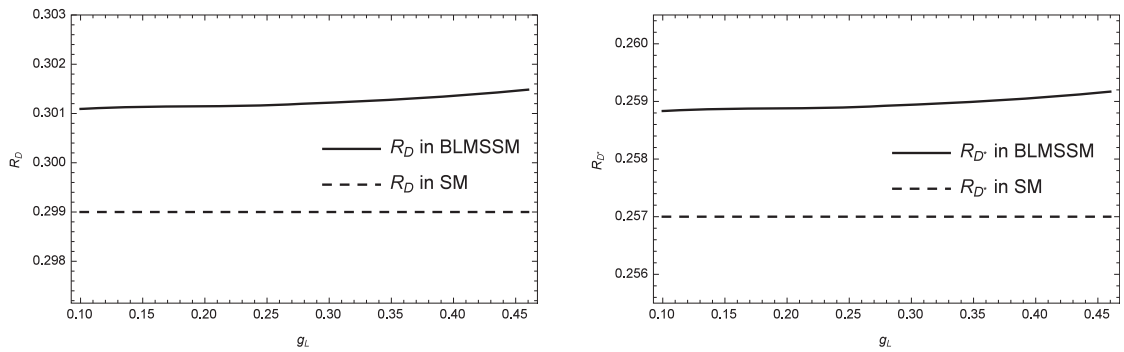


Fig. 4.  $R_D$  (left) and  $R_{D^*}$  (right) versus  $g_L$ .

$g_L$  is the coupling constant of the vertexes  $l\chi_L^0\tilde{L}$  and  $\nu\chi_L^0\tilde{\nu}$ . As a new parameter in the BLMSSM,  $g_L$  should affect  $R_{D^{(*)}}$ , which is of interest. The obtained numerical results are plotted in Fig. 4. The left-hand diagram shows  $R_D$  and the right-hand diagram shows  $R_{D^*}$ .

From Fig. 4, we can see that  $R_D$  and  $R_{D^*}$  both increase gently with increasing  $g_L$ . This is easy to understand: larger  $g_L$  improves the effects from NP. In order to get larger theoretical values of  $R_{D^{(*)}}$ , we need to choose a larger  $g_L$ . After considering the reasonableness of the range of parameter  $g_L$ , we use  $g_L=0.45$ . In this case, our numerical results are further improved.

### 7.3 Effects of parameters $\tan\beta$ , $m_2$ and $\mu$ on $R_{D^{(*)}}$

We also research the effects of parameters  $\tan\beta$ ,  $m_2$  and  $\mu$  on  $R_{D^{(*)}}$ . With the supposition  $g_L = 0.45$ ,  $(m_{\tilde{L}}^2)_{11} = (m_{\tilde{R}}^2)_{11} = (m_{\tilde{L}}^2)_{22} = (m_{\tilde{R}}^2)_{22} = 5.5 \times 10^5 \text{ GeV}^2$ ,  $(m_{\tilde{L}}^2)_{33} = (m_{\tilde{R}}^2)_{33} = 3 \times 10^8 \text{ GeV}^2$ , and  $m_2 = \mu = M_\xi$ , we scan the parameters of  $M_\xi$  versus  $\tan\beta$  in Fig. 5.

All the points in Fig. 5 can make  $R_D$  ( $R_{D^*}$ ) reach 0.304 (0.261), and some particular points can bring  $R_D$  ( $R_{D^*}$ ) to 0.305 (0.262). The theoretical values are improved, but they are not as big as we expected. However, our results are still better than those in the SM. All of the above discussions only consider the central values in the SM. If we consider the uncertainty of SM predictions  $R_D = 0.299 \pm 0.003$  [5] and  $R_{D^*} = 0.257 \pm 0.003$  [5], our

theoretical value of  $R_D$  ( $R_{D^*}$ ) can reach 0.308 (0.265), when we take the biggest value of the SM prediction.

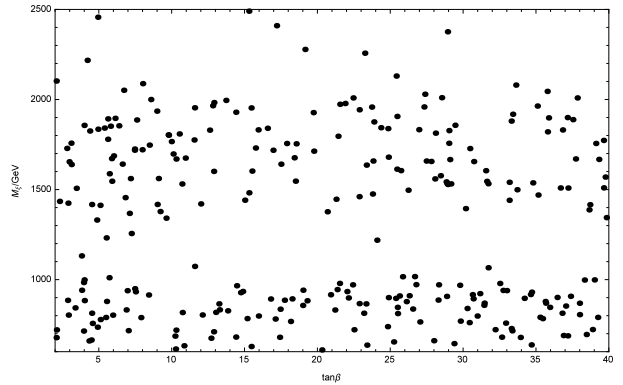


Fig. 5. The allowed parameters in the plane of  $M_\xi$  versus  $\tan\beta$  with  $g_L = 0.45$ ,  $(m_{\tilde{L}}^2)_{11} = (m_{\tilde{R}}^2)_{11} = (m_{\tilde{L}}^2)_{22} = (m_{\tilde{R}}^2)_{22} = 5.5 \times 10^5 \text{ GeV}^2$ ,  $(m_{\tilde{L}}^2)_{33} = (m_{\tilde{R}}^2)_{33} = 3 \times 10^8 \text{ GeV}^2$ .

## 8 Summary and future prospects

The SM cannot explain the experimental data for  $R_{D^{(*)}}$  well, so we hold that SM should be the low energy effective theory of a large model. We think the BLMSSM is promising for testing in the future. Compared with the MSSM, there are new particles and new parameters in the BLMSSM, and the new contributions

from these are the keys to solve the anomalies in  $R_{D^{(*)}}$ . For instance, the three lepton-neutralinos  $\chi_L^0$  are new particles in the BLSSM, and the Feynman diagram with  $\chi_L^0$  can give new contributions to  $R_{D^{(*)}}$ .

We find that the parameters  $(m_L^2)_{ii}$  and  $(m_R^2)_{ii}$  influence the theoretical results to some extent, and  $R_{D^{(*)}e}$  is approximately equal to  $R_{D^{(*)}\mu}$  only if there is a certain relationship between parameters  $(m_L^2)_{ii}$  and  $(m_R^2)_{ii}$ . After that, the effect of parameter  $g_L$  is important, and we can further raise theoretical values when it takes some appropriate values. Finally, using the central value of the SM prediction we scan the parameter space, and bring the value of  $R_D$  ( $R_{D^*}$ ) to 0.305 (0.262). Taking into account the SM uncertainty and adopting the biggest value in the SM, our result for  $R_D$  ( $R_{D^*}$ ) can reach 0.308 (0.265).

In this paper, we use effective field theory to compute  $R_{D^{(*)}}$  in the BLSSM. The one-loop corrections to  $R_{D^{(*)}}$  have an effect and the theoretical values can be increased (though they are not big improvements). We notice that the measurements of  $R_{D^*}$  (see Table 1) are not as large as the original measurements. This suggests that  $R_{D^*}$  perhaps is not so large. From the trend of experimental measurement, the experimental values of  $R_{D^{(*)}}$  might be smaller in the future. In fact, without considering this case, the measurement of  $R_D$  ( $R_{D^*}$ ) shows  $2.3\sigma$  ( $3.1\sigma$ ) deviation from its SM prediction, and our theoretical values are still better than the predictions given by SM. On the whole, the problem of  $R_D$  ( $R_{D^*}$ ) should be further researched both experimentally and theoretically in the future.

## Appendix

The formulae for the one-loop integral are:

$$\begin{aligned} \frac{(2\pi\kappa)^{4-D}}{i\pi^2} \int d^D p \frac{1}{(p^2-m_1^2)(p^2-m_2^2)(p^2-m_3^2)} &= -\frac{1}{\Lambda_{\text{NP}}^2} F_{11}(x_1, x_2, x_3), \\ \frac{(2\pi\kappa)^{4-D}}{i\pi^2} \int d^D p \frac{p^2}{(p^2-m_1^2)(p^2-m_2^2)(p^2-m_3^2)} &= \frac{1}{\varepsilon} -\gamma_E + \ln(4\pi\kappa^2/\Lambda_{\text{NP}}^2) + 1 - F_{21}(x_1, x_2, x_3), \\ \frac{(2\pi\kappa)^{4-D}}{i\pi^2} \int d^D p \frac{1}{(p^2-m_1^2)(p^2-m_2^2)(p^2-m_3^2)(p^2-m_4^2)} &= -\frac{1}{\Lambda_{\text{NP}}^4} F_{11}(x_1, x_2, x_3, x_4), \\ \frac{(2\pi\kappa)^{4-D}}{i\pi^2} \int d^D p \frac{p^2}{(p^2-m_1^2)(p^2-m_2^2)(p^2-m_3^2)(p^2-m_4^2)} &= -\frac{1}{\Lambda_{\text{NP}}^2} F_{21}(x_1, x_2, x_3, x_4), \end{aligned}$$

$$\begin{aligned} F_{11}(x_1, x_2, x_3) &= \frac{x_1 \ln x_1}{(x_1-x_2)(x_1-x_3)} + \frac{x_2 \ln x_2}{(x_2-x_1)(x_2-x_3)} + \frac{x_3 \ln x_3}{(x_3-x_1)(x_3-x_2)}, \\ F_{21}(x_1, x_2, x_3) &= \frac{x_1^2 \ln x_1}{(x_1-x_2)(x_1-x_3)} + \frac{x_2^2 \ln x_2}{(x_2-x_1)(x_2-x_3)} + \frac{x_3^2 \ln x_3}{(x_3-x_1)(x_3-x_2)}, \\ F_{11}(x_1, x_2, x_3, x_4) &= \frac{x_1 \ln x_1}{(x_1-x_2)(x_1-x_3)(x_1-x_4)} + \frac{x_2 \ln x_2}{(x_2-x_1)(x_2-x_3)(x_2-x_4)} \\ &\quad + \frac{x_3 \ln x_3}{(x_3-x_1)(x_3-x_2)(x_3-x_4)} + \frac{x_4 \ln x_4}{(x_4-x_1)(x_4-x_2)(x_4-x_3)}, \\ F_{21}(x_1, x_2, x_3, x_4) &= \frac{x_1^2 \ln x_1}{(x_1-x_2)(x_1-x_3)(x_1-x_4)} + \frac{x_2^2 \ln x_2}{(x_2-x_1)(x_2-x_3)(x_2-x_4)} \\ &\quad + \frac{x_3^2 \ln x_3}{(x_3-x_1)(x_3-x_2)(x_3-x_4)} + \frac{x_4^2 \ln x_4}{(x_4-x_1)(x_4-x_2)(x_4-x_3)}. \end{aligned}$$

## References

- 1 J. A. Bailey et al (MILC collaboration), Phys. Rev. D, **92**(3): 034506 (2015)
- 2 D. Bigi and P. Gambino, Phys. Rev. D, **94**(9): 094008 (2016)
- 3 H. Na, C. M. Bouchard, G. P. Lepage, C. Monahan, and J. Shigemitsu (HPQCD collaboration), Phys. Rev. D, **92**(5): 054510 (2015)
- 4 Debjyoti Bardhan et al, JHEP, **1701**: 125 (2017)
- 5 F. U. Bernlochner, Z. Ligeti et al, Phys. Rev. D, **95**(11): 115008 (2017)
- 6 S. Fajfer, J. F. Kamenik, and I. Nisandzic, Phys. Rev. D, **85**: 094025 (2012)
- 7 J. P. Lees et al (BaBar collaboration), Phys. Rev. Lett., **109**:

- 101802 (2012)
- 8 J. P. Lees et al (BaBar collaboration), Phys. Rev. D, **88**(7): 072012 (2013)
- 9 M. Huschle et al (Belle collaboration), Phys. Rev. D, **92**(7): 072014 (2015)
- 10 <http://www.slac.stanford.edu/xorg/hfag/semi/fpcp17/RDRDs.html>
- 11 R. Aaij et al (LHCb collaboration), Phys. Rev. Lett., **115**(11): 111803 (2015)
- 12 A. Abdesselam et al (Belle collaboration), Phys. Rev. D, **94**(7): 072007 (2016)
- 13 S. Hirose et al (Belle collaboration), Phys. Rev. Lett., **118**(21): 211801 (2017)
- 14 R. Aaij et al (LHCb collaboration), Phys. Rev. Lett., **120**(17): 171802 (2018)
- 15 R. Alonso, B. Grinstein, and J. Martin Camalich, Phys. Rev. Lett., **118**(8): 081802 (2017)
- 16 U. Nierste, S. Trine, and S. Westhoff, Phys. Rev. D, **78**: 015006 (2008)
- 17 A. Datta, M. Duraisamy, and D. Ghosh, Phys. Rev. D, **86**: 034027 (2012)
- 18 Y. Sakaki and H. Tanaka, Phys. Rev. D, **87**: 054002 (2013)
- 19 A. Crivellin, C. Greub, and A. Kokulu, Phys. Rev. D, **86**: 054014 (2012)
- 20 D. Choudhury, D. K. Ghosh, and A. Kundu, Phys. Rev. D, **86**: 114037 (2012)
- 21 A. Celis, M. Jung, X. Q. Li, and A. Pich, JHEP, **01**: 054 (2013)
- 22 I. Dorsner, S. Fajfer, N. Kosnik, and I. Nisandzic, JHEP, **11**: 084 (2013)
- 23 M. Duraisamy and A. Datta, JHEP, **09**: 059 (2013)
- 24 P. Biancofiore, P. Colangelo, and F. De Fazio, Phys. Rev. D, **87**: 074010 (2013)
- 25 M. Duraisamy, P. Sharma, and A. Datta, Phys. Rev. D, **90**: 074013 (2014)
- 26 M. Freytsis, Z. Ligeti, and J. T. Ruderman, Phys. Rev. D, **92**: 054018 (2015)
- 27 A. Greljo, G. Isidori, and D. Marzocca, JHEP, **07**: 142 (2015)
- 28 Y. Sakaki, M. Tanaka, A. Tayduganov, and R. Watanabe, Phys. Rev. D, **91**(11): 114028 (2015)
- 29 M. Tanaka and R. Watanabe, Phys. Rev. D, **87**(3): 034028 (2013)
- 30 W. S. Hou, Phys. Rev. D, **48**: 2342-2344 (1993)
- 31 M. Tanaka, Z. Phys. C, **67**: 321-326 (1995)
- 32 K. Kiers and A. Soni, Phys. Rev. D, **56**: 5786-5793 (1997)
- 33 P. Ko, Y. Omura, and C. Yu, JHEP, **1303**: 151 (2013)
- 34 R. Alonso, B. Grinstein, and J. Martin Camalich, JHEP, **1510**: 184 (2015)
- 35 R. Barbieri, G. Isidori, A. Pattori, and F. Senia, Eur. Phys. J. C, **76**(2): 67 (2016)
- 36 P. F. Perez and M. B. Wise, JHEP, **1108**: 068 (2011)
- 37 P. F. Perez and M. B. Wise, Phys. Rev. D, **82**: 011901 (2010)
- 38 Ryoutaro Watanabe, Phys. Lett. B, **776**: 5-9 (2018)
- 39 S. Dimopoulos, L. J. Hall, Phys. Lett. B, **207**: 210-216 (1988)
- 40 R. Barbieri and A. Masiero, Nucl. Phys. B, **267**: 679-689 (1986)
- 41 T. F. Feng, S. M. Zhao, H. B. Zhang et al, Nucl. Phys. B, **871**: 223-244 (2013)
- 42 S. M. Zhao, T. F. Feng, B. Yan et al, JHEP, **10**: 020 (2013)
- 43 S. M. Zhao, T. F. Feng, X. J. Zhan et al, JHEP, **07**: 124 (2015)
- 44 S. M. Zhao, T. F. Feng, H. B. Zhang et al, Phys. Rev. D, **92**(11): 115016 (2015)
- 45 F. Sun, T. F. Feng, S. M. Zhao et al, Nucl. Phys. B, **888**: 30-51 (2014)
- 46 X. X. Dong, S. M. Zhao, H. B. Zhang et al, Chin. Phys. C, **40**(9): 093103 (2016)
- 47 Y. Sakaki, M. Tanaka, A. Tayduganov, and R. Watanabe, Phys. Rev. D, **88**(9): 094012 (2013)
- 48 A. Datta, M. Duraisamy, and D. Ghosh, Phys. Rev. D, **86**: 034027 (2012)
- 49 M. Bohm, H. Spiesberger, and W. Hollik, Fortsch. Phys., **34**: 687 (1986); K. I. Aoki, Z. Hioki, R. Kawabe et al, Prog. Theor. Phys., **64**: 707 (1980); **65**: 1001 (1981); Prog. Theor. Phys. Suppl., **73**: 1 (1982)
- 50 W. Hollik, E. Krans, M. Roth et al, Nucl. Phys. B, **639**: 3 (2004); A. Denner, Fortsch. Phys., **41**: 307 (1993)
- 51 S. M. Zhao, T. F. Feng, H. B. Zhang et al, Chin. Phys. C, **37**(5): 053101 (2013)
- 52 C. Patrignani et al (Particle Data Group), Chin. Phys. C, **40**: 100001 (2016)
- 53 Albert M Sirunyan et al (CMS Collaboration), Submitted to: Phys. Lett., arXiv:1806.05264